Article

Where does the explosive energy in rock blasting rounds go?

Ouchterlony Finn*†, Nyberg Ulf*, Olsson Mats*, Bergqvist Ingvar**††, Granlund Lars**, and Grind Henrik***

*Swedish Blasting Research Centre at Luleå Univ. of Technology (Swebrec at LUT), Box 47047, S-10074 Stockholm, Sweden,
† corresponding author: finn.ouchterlony@ltu.se

**Dyno Nobel Europe AB, S-71382 Nora, Sweden,
†† corresponding author: ingvar.bergqvist@eu.dynonobel.com

***Nordkalk AB, Storugns, S-62034 Lärbro, Sweden,
e-mail: henrik.grind@nordkalk.com

Received: February 23, 2004 Accepted: March 12, 2004

Abstract

The energy partitioning of limestone production blasts has been measured under well controlled conditions; from rock properties determination, structural mapping and monitoring of drilling and charging, to VOD, 3D accelerometer and bench face movement measurements during the blast to postblast fragment size measurements. The efficiency of the transfer of energy from the charges to the surrounding rock has been estimated by introducing a new explosives test, the cylinder expansion test, which is discussed to begin with.

Hereby in-hole losses, seismic energy, kinetic energy of throw and fragmentation energy have been calculated. For the AN doped gassed bulk emulsion used in the quarry, it is estimated that 60-70 % of the explosive energy is transmitted to the rock, that the seismic and kinetic energy terms both amount to roughly 3-12 % and the fragmentation energy to less than 1-2 %. One candidate for the remaining losses, which are larger than the other three terms together, is the crushing of the blast-hole region. A rough estimate for the energy partitioning in bench blasting rounds is finally given.

1. Introduction

The company Nordkalk AB at Storugns on the island of Gotland is Scandinavia's largest producer of crushed limestone. Historically the amount of fines less than 25 mm in size has entailed a lower sales price or deposited on slag-heaps. There has been a continuous drive to lessen the amount of fines produced[1].

With the overall goal of decreasing the amount of fines produced by blasting, Nordkalk AB, Dyno Nobel Europe AB and Swedish Rock Engineering Research (SveBeFo) entered the EU-financed project *"Less fines production in aggregate and industrial minerals industry"*, project no. GRD-2000-25224 in 2001. "Less Fines" has other partners too, Montan-universität Leoben and ballast manufacturer Hengl Bitustein in Austria, the CGES & CGI departments of the Ecole de Mines in Paris, France and Universidad Politécnica de Madrid (UPM) with explosives manufacturer UEE and cement manufacturer Cementos Portland from Spain.

This article presents field tests made at the Klinthagen quarry of Nordkalk. During May 2002, 5 instrumented production rounds were blasted in order to measure where the explosive energy goes. The work is reported in greater detail[2) 3)]. These rounds were the basis for continued field-work during the spring of 2003 when Swebrec did the work on behalf of SveBeFo.

2. The energy balance of blasting

Detonating explosives form high pressure and temperature gases that can perform much work while they expand down to atmospheric pressure. The theoretically largest amount of work just about equals the detonation energy[4)]. Many manufacturers report a weight strength based on the related quantity explosion pressure E_0 or a lower value based on the assumption the the gases stop doing useful work at some pressure, e.g. 1000 atm. Langefors' weight strength[4)] is hardly used anymore.

Only a fraction η of the explosion energy is transferred to the rock mass. Some of this is converted to useful energy like kinetic energy of throw E_k and fragmentation E_f. Seismic energy E_s and other losses are also formed. The energy balance of a blast may thus be written

$$\eta \cdot E_0 = E_k + E_f + E_s + \text{other losses.} \quad (1)$$

Other losses are[5] the residual heat in the blast fumes, heat transferred to the rock mass, air shock waves and shock wave energy that doesn't result in fragmentation. Of these the residual heat and air shock waves are contained in the factor η of the left member of eq. 1. An example of losses in the rock mass is shock wave and friction losses in the crushed zone that surrounds the blast-hole.

The energy balance has been written on a form that shows what can be measured with reasonable work input. The kinetic, seismic and fragmentation energy components can be measured in the field. This article shows how this was done in the Klinthagen quarry.

3. On the work capacity of explosives

A new independent measure of the relative work capacity of explosives has been developed[6]. In the cylinder expansion test, copper tubes filled with explosives are shot and the explosive VOD and the expansion velocity of the tube wall are measured. In our tests, final wall velocities of 1100-1500 m/s were measured for civilian explosives in Ø 100/110 mm tubes. See Fig. 2. Other work[7) 8) 9)] was also helpful in developing the test method.

The event is fairly rapid. Within 40-50 μ s the wall accelerates and reaches a constant final velocity that is kept until the tube fractures. The event may be followed until the blast fumes have expanded about 8-9 times the original tube volume and more or less have stopped doing work on the copper cylinder.

The sum of the kinetic energy of the copper tube and the radial kinetic energy of the gases, the so called Gurney energy E_G, is computed. E_G is a measure of the work capacity of the explosive. The relative work capacity or the utilisation ratio is then given by

$$\eta = E_G/E_0. \quad (2)$$

Table 1 shows the measured values of some civil explosives[6]. ANFO prills from three different manufacturers were tested. One manufacturer also supplied an ANFO quality with 7 % of aluminium added. Titan® 6000 is the pure gassed SME bulk emulsion supplied by Dyno Nobel and used at Klinthagen. Titan 6080 contains 20 % of AN prills.

Em 682 is an AN/SN based emulsion explosive sensitises

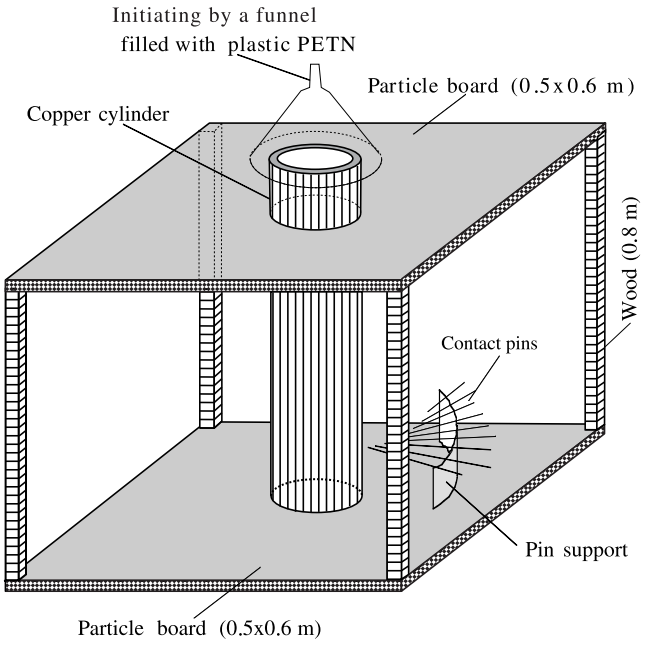

Fig. 1 Test set up for cylinder expansion test with i) wooden rig, ii) top initiation with plastic explosive and iii) contact pins. VOD is measured inside tube.

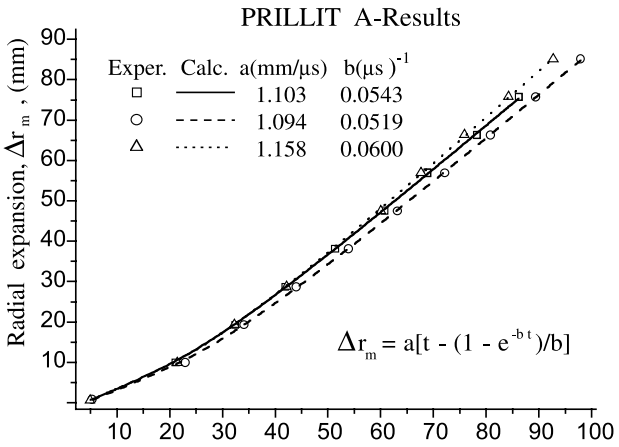

Fig.2 Expansion curve for ANFO (Prillit A), tube wall velocity versus time. a denotes the final wall velocity and 1/b is a measure of the acceleration phase.

Table 1 Data on the work capacity of civilian explosives.

Explosive	Density ρ kg/m^3	Final tube wall speed m/s	Explosion energy E_0 MJ/kg	Gurney energy E_G MJ/kg	Rel. work capacity η
ANFO	750-900	1100-1250	3.9-4.0	1.6-1.9	0.4-0.5
ANFO + alu	900	1400	5.1	2.5	0.5
Titan 6000	900	1200	3.2	1.8	0.5-0.6
Titan 6000	1150-1250	1300-1500	3.2	2.1-2.3	0.6-0.7
Titan 6080	800	1100-1200	3.3	1.8-2.0	0.5-0.6
Titan 6080	1150-1250	1400-1500	3.3	2.0-2.3	0.6-0.7
Em 682 100 %	1100-1200	1300	2.9	1.7-1.8	0.55-0.60
Em 682 80 %	1100-1200	1300	3.0	1.7-1.8	0.55-0.60

by glass micro-spheres. It is similar to many commercial explosives and was developed jointly by SveBeFo, Dyno Nobel AB and Kimit AB[10]. Em 682 contains 20 % of ANFO and 80 % of the emulsion by weight.

The most important conclusion from the data in Table 1 is that Titan 6080, despite the lower weight strength value given by Dyno, 3.3/4.0 = 84 %, performs more work than ANFO because the E_G-value is larger for Titan 6080 at a normal loading density of 1150 kg/m^3. The relative work capacity for the Titan series of explosives is 60-70 % but only 40-50 % for ANFO.

The table also show that the work capacity of the Titan series explosives increases with an increasing density despite that the VOD starts to drop when the density approaches 1300 kg/m^3. The consequence is that the VOD-value may not be a good measure of the work capacity of an explosive.

Adding AN or ANFO seems to have little influence on the work capacities of the emulsion explosives in Table 1. Nor are their acceleration phases very different either[6) 10)], except at the lowest densities, 800-900 kg/m^3.

Adding aluminium raises the work capacity of ANFO though but not the utilisation ratio η . The effect of aluminium is to prolong the acceleration phase during which the work is transferred considerably though[6)].

The ANFO and Titan tests were all made in Ø 100/110 mm tubes, i.e. tubes with an inner diameter of 100 mm and a wall thickness of 5 mm. For explosive E682, tubes with emulsion Ø 40/44, 60/66, 80/88 and 100/110 mm were tested, i.e. the explosive to metal mass ratio was in principle constant[10) 11)]. The work capacity of the explosive showed no significant influence of charge diameter despite the fact that the measured VOD-values did so, especially for E682 with 20 % emulsion. The same conclusions were drawn from tests on ANFO[12)].

The underwater test is another experimental measure of the work capacity of explosive[13)]. In comparison the cylinder test has several advantages:

1. The cylinder test has the same detonation geometry as in rock blasting, a grazing, axial stationary detonation in an extended charge.
2. It is easier to study the effect of charge diameter and e.g. decoupling in the cylinder test.
3. From the cylinder charge, about the same relative amount of explosive energy is transferred to the tube as from the blast-hole charge in rock blasting.
4. The explosive stops doing useful work in the cylinder test when the gases or fumes have expanded about 5-10 times, which is close to the limit of 10-20 times that several researchers consider valid in rock blasting[4)]. The charge in the underwater test continues doing work down to much greater expansion volumes[13)].
5. The energy in the cylinder test is partitioned much more like in rock blasting[6)].

In the test rounds at Klinthagen, Titan 6080 from a Dyno bulk truck, with a density of 1100-1200 kg/m^3 in Ø 89-mm holes, was used[14)]. Thus here a relative work capacity of about 60-70 % is used in the energy balance, corresponding to 30-40 % of in-hole losses.

Fig. 3 Muckpile after test round no. 1 in lower bench (bench 2).

4. The field conditions at Nordkalk's Klinthagen quarry.

The blasts at Klinthagen were single row rounds with 20-25, Ø 89-mm blast-holes, about 13 m deep, inclined at 16º and 2 m of sub-drilling in 11-m high benches. See Fig. 3. The nominal burden and spacing values were 3.6 and 4.8 m respectively. The charging length was on average slightly less than 10 m and the stemming consisted of about 3 m of gravel. The linear charge concentration was 7.4 kg/m for an average charge of 68 kg and specific charge of about ca 0.4 kg/m^3.

The Nonel Unidet® was used for initiation of the rounds, using a U475 cap in a 1.7 kg bottom primer and a U500 cap in a 1.25 kg charge at the top of the explosive column. The surface delays were either Unidet Snapline SL42 in three of the rounds or SL25 in the other two. No differences in blast results due the different surface delays were found.

The initiation accuracy is determined by the nominal scatter of the bottom caps, ±6 ms, and becomes in practice about ±9 ms between two caps. Our function control measurements gave the initiation statistics (mean ± scatter) 23.1 ± 6.0 ms and 43.3 ± 6.0 ms, which was considered fully acceptable.

The VOD measurements showed the characteristic pattern for gassed bulk emulsions, namely that the VOD is highest in the bottom of the charge column and decreases towards the top. We obtained the bottom results 4990 ± 260 m/s and 4410 ± 190 m/s at the top. This was also considered fully acceptable.

The quarrying at Nordkalk is done in two benches, Fig. 3. The limestone in the upper bench (level 1) of the test area consists of horizontally layered stromatoporiod and crinoid facies in the proportions 80/20. The lower bench consists mainly of reef, fragmentory and crinoid facies in the proportions 75/15/10. Differences in arrival times from ground vibration measurements were used to estimate the P-wave speed c_P in the benches. There was a considerable difference in the two benches, c_P = 4350 ± 550 m/s in the

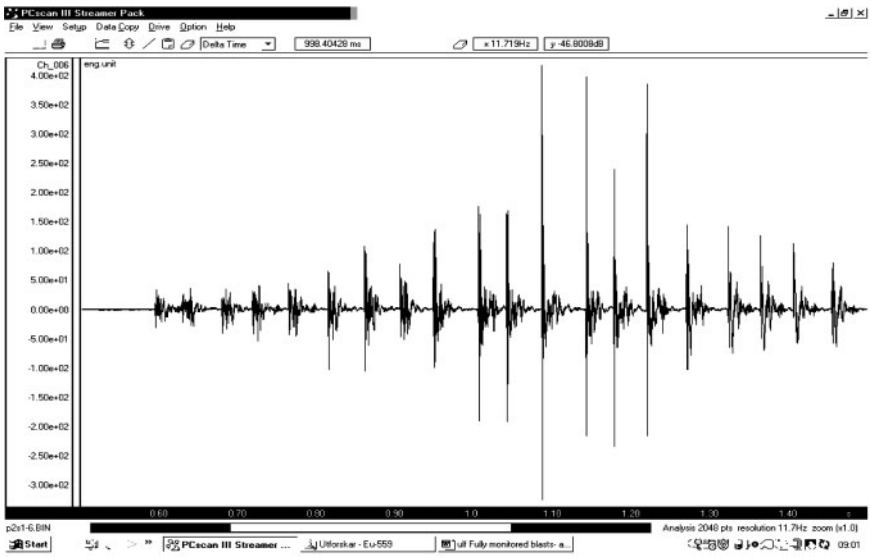

Fig. 4 Accelerometer signals from round no. 1, gauge point 2h. Twenty blast-holes.

upper and 5550 ± 700 m/s in the lower bench.

The test area lay in the South Eastern corner of the quarry. Two rounds behind each other were fired in the upper bench and three in the lower bench, some 300 m to the East in order to estimate the effect of limestone quality and geology. The rock masses had been structurally mapped and the in-situ fracture families had been determined by our French Less Fines colleagues, Moser[15].

Our Austrian colleagues had made thorough measurements of rock mechanics parameters, Moser[16] and also laboratory scale blasting tests[17].

We did thorough follow ups of the staking out, drilling and charging of the blast-holes during the test rounds together with our Nordkalk and Dyno colleagues. On top of the VOD we also measured i) the ground vibrations in order to calculate the seismic energy E_s during the blasts and ii) the bench face movement in order to calculate the kinetic throw energy E_k. We calculated the fragmentation energy E_f from the fragment size distribution measured after blasting.

5. Measurement and calculation of the energy components

5.1 Ground vibrations and seismic energy

Our experience tells us that surface mounted geophones can not reproduce the vibrations from blasting rounds accurately enough to e.g. determine blast damage in rock. The frequency contents are filtered and the surface mounting distorts the signal appreciably. We feared that these limitations would apply when measuring the seismic energy at Klinthagen.

Therefore we used dismountable three component accelerometers with steel anchors that were grouted to the bottoms of 4-m deep gauge holes. Three gauge holes were used in each bench. Two were positioned about 20 m behind the first round, i.e. row of holes, symmetrically with respect to and about 10 m from the centre line in order to compare the signals from equivalent hole positions. One gauge hole lay about 30 m behind the first row on the centre line in order to evaluate the geometric damping of the signals better. The measuring range was 10-50 m. The bandwidth 25 kHz of the recording equipment was determined by the DAT recorder SIR-1000 from Sony.

We thus recorded on nine channels during each round without signal losses. A trace is shown in Fig. 4. It may be seen that the individual pulses do not overlap and that they are distinct. The effect spectrum is fairly constant from 20-4000 Hz. Peak vibration velocities (PPV) were obtained after an integration and vector summation of three component signals.

The PPV-values were reasonable and tended to be larger in the upper bench, level 1. See Fig. 5. The PPV-values were normalised against the P-wave velocity c_P and the scaling law could be written

$$PPV = (0.047 \pm 0.02) \cdot c_P \cdot [\sqrt{(Q/68)}/R]^{2.09}. \quad (3)$$

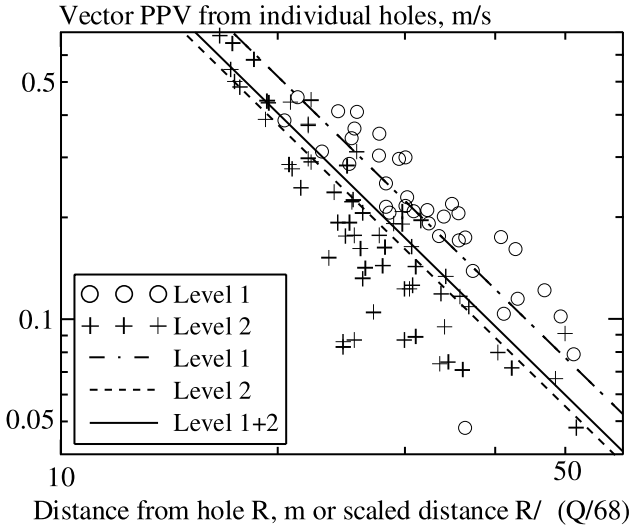

Fig. 5 Site scaling law for test area in Klinthagen quarry. log(PPV) as function of log(R/√Q), where R/√Q is reduce distance. Note the charge normalisation against average charge weight 68 kg per hole in test rounds. Level = bench.

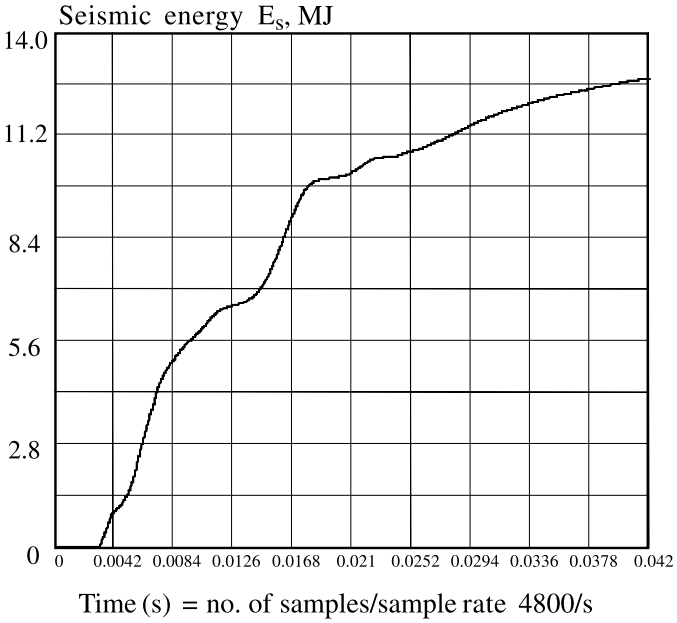

Fig. 6 Seismic energy radiated from hole no. 15 in round no. 1 versus time.

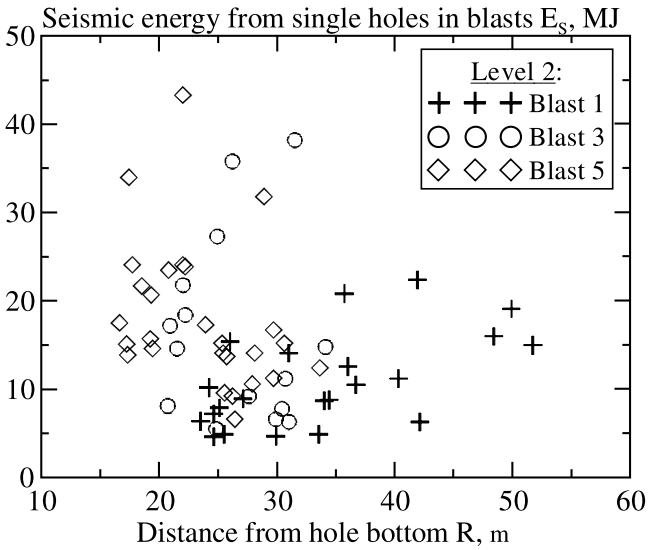

Fig. 7 Calculated values of seismic energy E_s for all holes in lower bench.

Here Q is the charge size in kg and R is the distance between charge and gauge in m. The value of the damping exponent is high, 2.09, and the scaling law should be checked before it is used outside the 10-50 m range. The calculated prefactor for bench 1 was 0.49 and for bench 2 0.045 but practically speaking 0.047 could be used in both benches as the difference is less than ±5 %.

An approximate seismic energy value E_s (J) may be calculated form the time trace of the vibration signal[18) 19)],

$$E_s(T) = 4\,\pi\,R^2 \cdot \rho c_P \cdot \int_0^T v_R^2(t)dt. \qquad (4)$$

R (m) is the distance between charge and gauge and $\rho \approx 2600$ kg/m^3 is the rock density. Eq. 4 doesn't account for a number of factors: an extended charge, wave reflections, a velocity vector that deviates from the normal of the wave front, outgoing and incoming waves, non-elastic material behaviour etc. The expression is thus seriously simplified but has a distance dependence so that $E_s(T)$ should be reasonably independent of dis-tance R when losses are small.

Luckily the single hole pulses in Fig. 4 do not overlap. The integration time can thus basically be restricted to either 25 or 42 ms. The $E_s(T)$ curves normally display a knee after about 20 ms, see Fig. 6. By then some 80 % of the seismic energy has radiated out. Our integrations were normally made considerably longer.

The diagram of E_s versus time in Fig. 7 displays a surprisingly large scatter, a factor of 9 roughly between the highest and the lowest values or 5-45 MJ per hole. Table 2 gives statistics for the data lumped with respect to gauge point, bench (level) and round. The average radiated seismic energy is somewhat higher from the holes in bench 1 than from the holes in bench 2, 20 MJ versus 15 MJ. The difference is hardly significant though, considering the large scatter in the data.

Factors that may contribute to the scatter in the calculated values are i) the layered limestone, ii) its anisotropy and iii) the fracturing around a blast-hole that influences the wave transmission from a neighbouring blast-hole. We didn't observe any effect of the direction of propagation of the waves. The wave shielding effect of fractures is also considered important[20)].

The uncertainty and the scatter of the seismic energy values made us use the global sta-tistics. For a blast-hole with Q = 68 kg of explosive we then obtain

$$E_s = 17 \pm 9\ \text{MJ/hole} = 0.25 \pm 0.13\ \text{MJ/kg explosive} = (0.075 \pm 0.040) \cdot E_0 \qquad (5)$$

when the explosion energy value of E_0 = 3.31 MJ/kg for Titan 6080 is used. In round numbers the seismic energy thus becomes $E_s/E_0 \approx$ 3-12 %.

Table 2 Statistics for radiated seismic energy from single blast-holes, E_s in MJ.

	Lower bench			Upper bench	
Gauge point	Round 1	Round 3	Round 5	Round 2	Round 4
1 or1'	8.5 ± 6.3	17.4 ± 12.0	25.1 ± 9.6	17.2 ± 4.5	15.4 ± 5.8
2 or2'	10.8 ± 4.7	10.1 ± 3.7	11.5 ± 3.0	15.2 ± 5.1	15.7 ± 2.8
3 or 3'	12.9 ± 5.2	19.3 ± 12.0	17.3 ± 4.3	29.9 ± 14.4	23.7 ± 4.6
Round	10.9 ± 5.4	16.2 ± 10.5	18.1 ± 8.2	20.8 ± 11.0	18.8 ± 5.8
Bench	15.2 ± 8.5(64)			20.1 ± 9.6(31)	

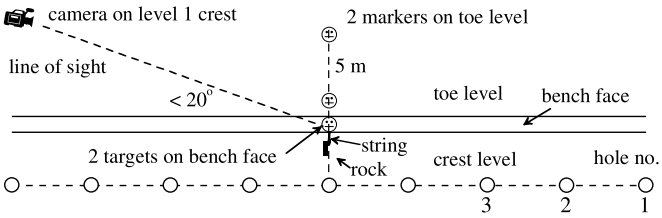

Fig. 8 Bird's eye view of the HSV set up for measurement of bench face motion.

5.2 Bench face velocity and kinetic energy

In order to measure the bench face motion we used a high-speed video (HSV), Red Lake MSD Motion Meter 1000 with max 1000 fps. The motion was analysed with the Blas-ter's MAS software from MREL. To obtain clear markers, two cardboard boxes were strung on a line from the top of the bench, 4 and 7 m below the crest respectively. See Fig. 8.

On the floor, two boxes were placed 5 m apart to give the length scale. The camera was placed about 300 m from the blast with a near grazing angle to the face, less than 20°, to minimise the angle errors.

The box markers moved with a relatively constant velocity the first 0.25 s and were tracked about twice as long, see Fig. 9. The velocity vectors of the tracked points show a normal bulging face. We measured face velocities in the range 8.5-11.3 m/s. The burden varied somewhat from round to round but there was no systematise correlation with the face velocity.

An assumption about the velocity distribution $V(x,y)$ in the moving rock mass is needed in order to calculate the kinetic energy. An upper limit is obtained if the velocity is assumed to be constant within the burden. This could be reasonable initially but hardly for any longer period of time for a muckpile that is in contact with the new face as in Fig. 3. This gives

$$E_k = \int {}^1\!/_2 MV^2 = {}^1\!/_2 \rho \cdot S\iint V^2(x,y)\mathrm{d}x\mathrm{d}y < \rho \cdot SBH \cdot V^2{}_{i,\max}. \quad (6)$$

M is the rock mass per hole, H (m) bench height, B (m) burden and S (m) the spacing.

The form of the muckpile probably corresponds better to a velocity distribution that is zero at the blastholes and increases linearly towards the face in horizontal direction. With no vertical variation the kinetic energy is reduced to a 1/3 of the maximum value in eq. 6. This is an approximate lower limit for the kinetic energy. Retardation effects caused by block collisions in space could e.g. explain the

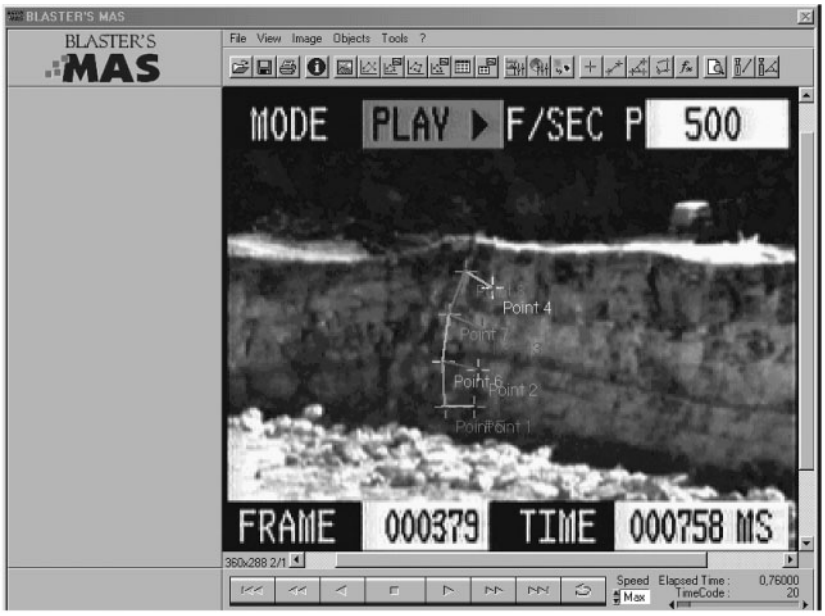

Fig. 9 High-speed image from round no. 4, about 100 ms after face starts to move.

Table 3 The calculated values for the kinetic energy, E_k per blast-hole.

	Lower bench			Upper bench	
	Round 1	Round 3	Round 5	Round 2	Round 4
Initial velocity, m/s	10.1	10.7	8.6	-	11.1
- bench height, m	10.5	11.0	10.1	-	8.4
- volume, m^3/hole	182.6	191.3	175.6	-	146.1
Maximum E_k, MJ	24.2	28.5	16.9	-	23.4
Minimal E_k, MJ	8.1	9.5	5.6	-	7.8
E_k variation, MJ		5.6 − 28.5		7.8 − 23.4	
Q charge, kg/hol	68	74	71	-	59
E_k/Q, MJ/kg		0.08 − 0.39		0.13 − 0.40	
E_k/E_0, %		2.4 − 11.6		4.0 − 12.0	

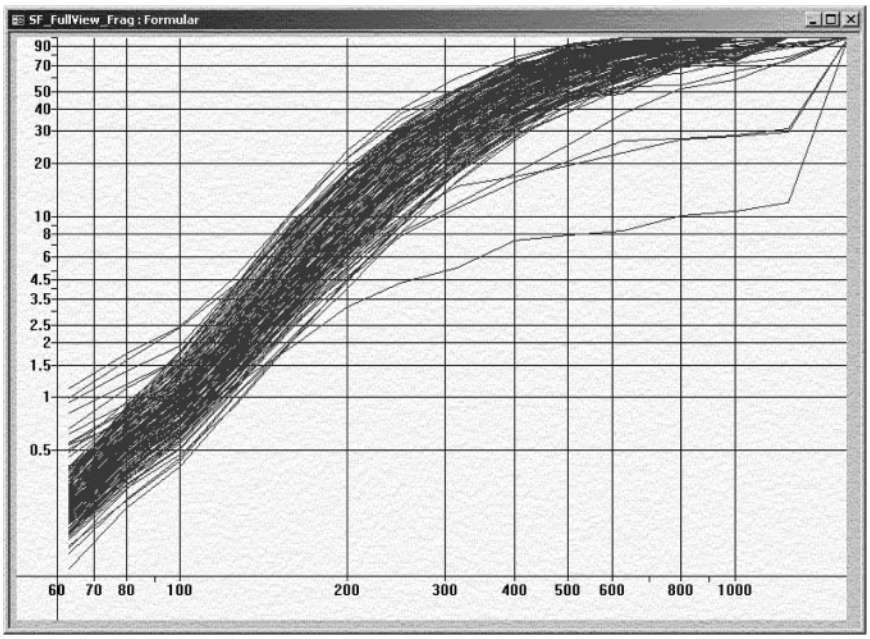

Fig. 10 Fragment size distributions from truckloads from round no. 4, level 1.

span in values.

The calculated values for the kinetic energy are shown in Table 3.

Thus we may estimate the kinetic energy of the test rounds at Klinthagen to about as large as the seismic energy, i.e. 3-12 % of the explosion energy.

A closer study of the bench face movement in the two other quarries that participate in the Less Fines project has been made[21] , the amphibolite quarry of Hengl Bitustein and the limestone pit of Cementos Portland (CP). The estimates of the kinetic energy have the same uncertainties and are 5-16 % for Hengl and 2.5-7 % for CP.

5.3 Fragment size distribution and fragmentation energy

The fragmentation energy consists of the energy supplied when new surfaces are created. Starting from the fragment size distribution (cumulative mass passing versus screen size) and an assumption on fragment shape, the total area of the muck pile may be roughly calculated.

Nordkalk has installed digital equipment to measure the fragments size distribution at the primary crusher. Every truckload is photographed by a video camera on a frame with lighting before it is dumped into the crusher. The system keeps track of whether the truck comes from the upper or the lower bench. One round may consist of several hundred truck loads, see Fig. 10.

Normally the image analysis will not resolve pieces smaller than 1/20 of the largest rock in the image well. At Nordkalk the resolution limit is about 50 mm, which is higher than the fines limit 25 mm. Therefore a second video camera, with a resolution of 10 mm is installed over the belt after the primary crusher. It can thus measure the combined amount of fines that blasting and crushing creates before the material is fed into the processing plant. These data are however not directly suitable for estimating the blasted size distribution.

We have used the cumulative Rosin-Rammler distribution to describe the fragmentation

$$P(x) = 100 \cdot [1 - 2^{-(x/x_{50})^n}]. \quad (7)$$

Here x_{50} is the screen size through which 50 % of the fragments pass and the uniformity index n is a measure of the slope of the curve. Assuming that there are N_h holes in the row, its volume becomes $V_0 \approx N_h \cdot SBH$. For reasonably cubic fragments within a size interval Δx around the side length x, their number ΔN_b and the corresponding surface area ΔA are related by $\Delta A = \Delta N_b \cdot 6x^2 = 6V_0 \cdot P'(x)/x \cdot \Delta x$. An integration over all fragment sizes yields

$$A_{round} = 6V_0/x_{50} \cdot (\ln 2)^{1/n} \cdot \Gamma(1\text{-}1/n). \quad (8)$$

The gamma function $\Gamma(1\text{-}1/n)$ has a finite value as long as $n > 1$. The basic estimate of the surface area of the

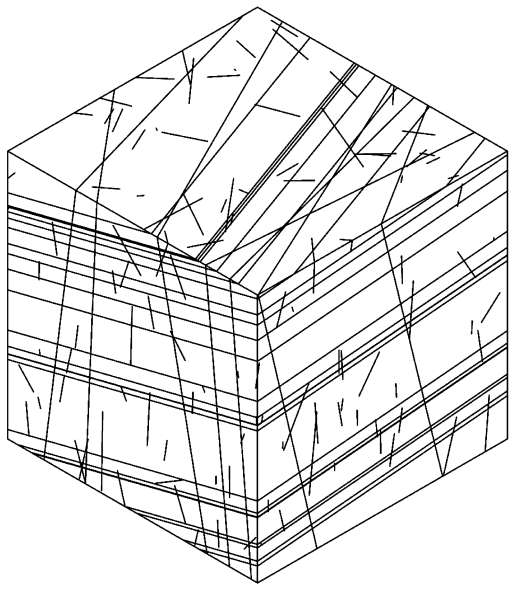

Fig. 11 Fractures in a Simbloc simulation for fragmentory limestone[15].

Table 4 Calculation of fragmentation energy in test rounds.

	Upper bench			Lower bench	
	Round 1	Round 3	Round 5	Round 2	Round 4
V_0, m^3	3 468.9	3 442.8	4 214.9	3 651.5	3 067.2
$A_{\text{in-situ}}/V_0$, m^2/m^3	2.78	2.78	2.78	5.97	5.97
$E_{\text{f,in-situ}}$, MJ	1.31	1.30	1.59	6.10	5.13
round x_{50}, m	0.48	0.41	0.42	0.43	0.41
$6V_0/x_{50}$, m^2	43 181	50 383	59 785	50 951	45 107
A_{round}/V_0	20.1	23.0	20.6	22.1	21.9
A_{new}/V_0, m^2/m^3	17.3	20.2	17.8	16.1	15.9
$E_{\text{f,round}}$, MJ	9.88	11.22	12.30	11.18	9.31
E_f, MJ	8.57	9.92	10.71	5.08	4.19
E_f/Q, MJ/kg	0.0063	0.0071	0.0060	0.0033	0.0032
E_f/E_0, %	0.19	0.21	0.18	0.10	0.10

muckpile thus becomes $6V_0/x_{50}$ and it is modified somewhat by the value of n.

Some of the surfaces in the muckpile are not new, they existed already in-situ. To distinguish between the fresh and in-situ surfaces in the muckpile is hardly practicable. Therefore we utilised the structural mapping made and an ensuing simulation, see Fig. 11, to estimate the existing area in-situ[15]. Equation 8 with in-situ data has been used to compute $A_{\text{in-situ}}$.

If we further know the specific surface energy γ (J/m^2), required to create fracture surfaces, then we may calculate the fragmentation energy as

$$E_f = A_{\text{new}}\cdot\gamma = (A_{\text{round}}-A_{\text{in-situ}})\cdot\gamma = E_{\text{f,round}}-E_{\text{f,in-situ}} \quad (9)$$

The surface energy may be measured either in the form of the Rittinger coefficient R (m^2/J) or of the fracture toughness K_{Ic} (Pa$\sqrt{}$m). Both quantities were measured for the rocks of the Less Fines project[17] and they yield quite similar γ-values. Here we have used $\gamma = 1/R$, which roughly is abut 100-150 J/m^2.

Table 4 shows that about 15-20 m^2 of surface per m^3 of intact rock was created. The in-situ fracturing is larger in the upper bench (level 1), about 6.0 m^2/m^3, than in the lower one, 2.8 m^2/m^3. The blasting seem to create less new surface in the upper bench though so the total surface in the upper bench muckpiles becomes 22.0 m^2/m^3 and 21.2 m^2/m^3 in the lower bench muckpiles, i.e. in practice the same!

Converted to fragmentation energy the result becomes 3.3 kJ/kg in the upper bench and 6.5 kJ/kg in the lower. This corresponds to the negligible amounts 0.1-0.2 % of the explosion energy 3.31 MJ/kg!

6. The measured components of the energy balance

The energy components that have been computed from the measurements in the Klinthagen quarry may now be entered into the energy balance of eqn. 1. The results are shown in Table 5 together with data from the other quarries in the Less Fines project[15] and literature data[18) 22].

It is striking that the loss term makes up about half or more of the work transferred from the explosive to the rock mass at the first three sites. As already mentioned, the residual heat of the blast fumes and the air shock waves are already contained in the utilisation ratio η, as is the axial kinetic energy of the fumes.

Our colleagues[23] give a slightly different explanation. The show that by assuming an incomplete chemical reaction $\eta < 1$, the can with reasonable accuracy calculate the expansion curves of the cylinder tests. Both explanations are probably needed in order to give an accurate picture of the process in the blast-hole.

The values for the seismic and kinetic energies were given with broad intervals. The correctness of the fragmentation energy hinges on how well $P(x)$ describes the fragment size distribution in the fines range.

There are unfortunately many indications that the Rosin-Rammler distribution gravely underestimates the number of fragments smaller than say 5 mm[24]. There are further few cases of screened full size blasts.

One such case is the Bårarp rounds[25) 26]. There are several screened distributions that cover the range 0,074-1000 mm. An estimate[17] is that 70-80 % of the fracture surface is made up of fragments smaller than 0,1 mm and 90 % of fragments smaller than 1 mm. Therefore the fines part of the distribution is essential when calculating the fragmen-

Table 5 Energy balances of blast rounds at different sites.

Site	No. of rounds	$\eta\cdot E_0$ %	E_s %	E_k %	E_f %	Losses in rock, %
Klinthagen	5	60-70	3-12	3-12	0.1-0.2	38-53
La Concha	2	40-50	2-6	16-25	0.1-3.2	16-22
Eibenstein	2	~ 65	0.4-2.5	6-27	-	35-58
Spathis[22]	1	58	5	27	0.3	26
Hinzen[18]	5	-	0.1-5	-	-	-

tation energy.

This makes it possible that the amount fresh fractures surface created by the blast could have been underestimated by say up to a factor of 10. Even if that were the case, it would only amount to 1-2 % of the explosive energy. Simply stated, it seems that fragmentation energy in any case is less than the margin of error of the other energies.

Heat deposited in the rock is another possible energy loss. It has several parts, e.g. shock wave heating, friction work during crushing of the rock around the blast-hole and heat transfer from the blast fumes that flow in the widening fractures.

There is evidence that the crushing work may be considerable. An analogy with projectile penetration[27] gives the number 1 kJ/cm^3 = 1 GJ/m^3 for hole expansion. If the blast-hole is expanded to twice its original size during crushing, a Ø 89 mm blasthole with the volume 6.2 *l*/m consumes about 6.2 MJ. The hole itself contains 7.4 kg of explosive. The crushing work would then be 0.84 MJ/kg or about 25 % of the explosion energy. This term is of the right order compared to the loss term 38-53 % at Klinthagen in Table 5.

An estimate based on Bond's equation[28], with a work index W_i of about 10 kWh/ton, crushing the rock down to an x_{80} of 100 µ m, says that this would require about 10 kWh/ton or 10 MJ/m^3. This is two orders of magnitude smaller than the penetration number above. The difference is that Bond's equation describes crushing or grinding under atmospheric conditions, not under a high blast pressure.

Another indirect piece of evidence is half-scale blasting tests with Ø 20 mm charges in granite to determine the maximum burden[29]. Putting the charge in a hole of double the charge volume permitted the charge to break out a larger burden than when the charge was in direct contact with the blast-hole wall. Accepting crushing around the blast-hole as the major energy loss in blasting requires more direct evidence though.

7. Conclusion

The measurements made at Nordkalk's Klinthagen quarry and at the other sites of Table 5 show that a rough description of the energy partitioning of a blast with bulk emulsion explosives would be

- Crushing and other losses in the rock mass 20 – 40 %
- Kinetic energy of throw 10 – 20 %
- Seismic energy 5 – 10 %
- Fragmentation energy 0.1 – 2 %

The calculated kinetic energy varies by at least a factor of three, the measured seismic energy for a whole round by at least a factor of two. The fragmentation energy, even with the blasting fines included, lies well within the uncertainties of the other two components! There is some evidence to say that crushing around the blasthole is the dominating energy loss. This is hard to measure in the field though.

What has been gained by this energy balance approach, by showing that the energy required to create the fresh fracture surfaces in a muckpile makes up for an insignificant part of the explosive energy?

- Firstly, within the Less Fines project, we conclude that the energy balance hardly is a viable approach to minimise the amount fine material created by blasting.
- Secondly we believe that a deeper understanding of the energy transfer from explosive to rock through the zone surrounding the blasthole carries the possibility of improving the blasting process. Swebrec ha initiated work where extended cylinder tests hopefully will shed light on this.

Acknowledgements

The authors want to express their gratitude to the production personnel at Nordkalk and Dyno Nobel for providing excellent help in this investigation and in other investigations within the Less Fines project.

References

1) Kattilavaara, N. Decrease in amount of fines < 25 mm at Nordkalk Storugns AB in the Storugns limestone quarry on Gotland. In *Proc Discussion meeting BK –95*, pp 128-140. Swedish Rock Construction Committee 1995. In Swedish.
2) Ouchterlony, F, U Nyberg, M Olsson, I Bergqvist, L Granlund & H Grind. The energy balance of production blasts at Nordkalk's Klinthagen quarry. In *Proc EFEE 2nd World Conf Expl & Blasting Techn*, R Holmberg ed, pp 193-203. Balkema 2003.
3) Ouchterlony, F, U Nyberg, M Olsson, I Bergqvist, L Granlund & H Grind. Where does the energy in blasting rounds go? Accepted for publication *Proc Discussion meeting BK 2004*, Swedish Rock Construction Committee 2004. In Swedish.
4) Persson, P-A, R Holmberg & J Lee. *Rock Blasting and Explosives Engineering*. CRC Press, Boca Raton FL 1994.
5) Vestre, J. The work capacity of explosives under critical conditions, with reference to energy measurements during under water blasting. In *Sprängämnens verkan-segenskaper*, Nordic conference, pp 35-61. Swedish Detonic Research Foundation, SveDeFo, Stockholm 1987. In Norwegian.
6) Nyberg, U, I Arvanitidis, M Olsson & F Ouchterlony. Large size cylinder expansion tests on ANFO and gassed bulk emulsion explosives. In *Proc EFEE 2nd World Conf Expl & Blasting Techn*, R Holmberg ed, pp 181-191. Balkema 2003.
7) Souers, P C & L C Haselman Jr. Detonation Equation of state at LLNL. 1993. Lawrence Livermore National Laboratory report UCRL-ID-116113. NTS, Springfield VA 1994.
8) Helte, A, H Almström, G Andersson, S Karlsson & J Lundgren. Evaluation of experiments conducted on the explosive B2211D at FOA. I: Energy Equations for the inert explosive and the reaction products. Report FOA-R—99-01142-310-SE. Swedish Defence Research Agency FOI, Stockholm 1999. In Swedish.
9) Trzciński W A & S Cudziło. The application of the cylinder test to determine the energy characteristics of industrial explosives. *Archives of Mining Sciences* v 46(3), pp 291-307. 2001.
10) Nie, S, J Deng & F Ouchterlony. Expansion work from an emulsion explosive in a blast-hole – measurements and simulations. SveBeFo rpt 48. Swedish Rock Engineering Research, Stockholm 2000. In Swedish.
11) Arvanitidis, I, U Nyberg & F Ouchterlony. The diameter effect on detonation properties of cylinder test experiments with emulsion E682. SveBeFo report manuscript. Swedish Rock Engineering Research, Stockholm 2004.
12) Davis, L L & L G Hill. ANFO cylinder tests. In *Shock Compression of Condensed Matter – 2001*, M D Furnish, N N Thadhani & Y Horie eds, pp 165-168. American Institute of Physics 2002.

13) Bjarnholt, G. Suggestions on standards for measurement and data evaluation in the underwater explosion test. *Propellants, Explosives, Pyrotechnics* v 5, pp 67-74. 1980.
14) Haslinger, I & N Nilsson. Blasting experiences from the introduction of gassed bulk emulsion on Gotland. In *Proc Discussion meeting BK 2000*, pp 121-127. Swedish Rock Construction Committee 2000. In Swedish.
15) Moser, P. Less Fines production in aggregate and industrial minerals industry. In *Proc EFEE 2nd World Conf Expl & Blasting Techn*, R Holmberg ed, pp 335-343. Balkema 2003.
16) Moser, P. Mechanical fragmentation tests – Optimised comminution sequence - Energy register functions. Less Fines techn rpt no 22. EU-project no GRD-2000-25224. 2002.
17) Moser, P, A Grasedieck, J du Mouza & E Hamdi. Breakage energy in rock blasting. In *Proc EFEE 2nd World Conf Expl & Blasting Techn*, R Holmberg ed, pp 323-334. Balkema 2003.
18) Hinzen, K-G. Comparison of seismic and explosive energy in five smooth blasting test rounds. *Int J Rock Mech Min Sci* v 35 no 7, pp 967-967. 1998.
19) Achenbach, J D. *Wave Propagation in Elastic Solids*. North Holland 1973.
20) Blair, D P & L W Armstrong. The spectral control of ground vibration using electronic delay detonators. *Int J for Blasting and Fragmentation* v 3 no 4, pp 303-334. 1999.
21) Segarra, P, J A Sanchidrián, L M Lopéz, J A Pascual, R Ortiz, A Gómez & B Smöch. Analysis of bench face move ment in quarry blasting. In *Proc EFEE 2nd World Conf Expl & Blasting Techn*, R Holmberg ed, pp 485-495. Balkema 2003.
22) Spathis, A T. On the energy efficiency of blasting. In *Proc 6th Int Symp on Rock Fragmentation by Blasting*, pp 81-90. Symposium series S21. SAIMM Johannesburg 1999.
23) Sanchidrián, J A & L Lopéz. Calculation of explosives useful work. In *Proc EFEE 2nd World Conf Expl & Blasting Techn*, R Holmberg ed, pp 357-361. Balkema 2003.
24) Ouchterlony, F. 'Bend it like Beckham' or a simple yet far-ranging fragment size distribution for blasted and crushed rock. Less Fines techn rpt manuscript. EU-project no. GRD-2000-25224. 2003.
25) Olsson, M & I Bergqvist. Fragmentation in quarries. In *Proc Discussion meeting BK 2002*, pp 31-38. Swedish Rock Construction Committee 2002.
26) Moser, P, M Olsson, F Ouchterlony & A Grasedieck. Comparison of the blast fragmentation from lab-scale and full-scale tests at Bårarp. In *Proc EFEE 2nd World Conf Expl & Blasting Techn*, R Holmberg ed, pp 449-458. Balkema 2003.
27) Szendrei, T & C V A Cunningham. Cavity expansion by hypervelocity impact ap-plied to blasthole expansion by detonation. In *Proc ISEE 30th Ann Conf Expl & Blasting Tech*. ISEE, Cleveland OH. 2004.
28) Bond, F C. The third theory of comminution. *Mining Engineering*, May, pp 484-494. 1952.
29) Persson, P-A, A Ladegaard-Pedersen & B Kihlström. The influence of borehole diameter on the rock blasting capacity of an extended explosive charge. *Int J Rock Mech Min Sci* v 6, pp 277-284. 1968.